room for interpretation and generalization whenever necessary. Presently, ε includes uncertainties due to line centre-to-pixel centre position, window choice in the gaussian fitting (up to 7 pixels), FWHM of the PSF (up to 2 pixels). ε is provisionally set to a predefined code when there is *empirical* evidence for blending with argon lines. Blends with weaker argon lines undoubtedly remained unrecognized, especially above 4700 Å where the empirical test turned out to be less sensitive (among others due to the undersampling of the lines in the available frames).

At present, however, the user will have to specify his (own) global dispersion fit function using the possibility offered by MIDAS to define user functions, and he will himself have to take care of the transport of the coefficients in the system during the further reductions. Nevertheless, ESO is looking into the possibility to include the alternative of global dispersion formulae in future versions of the echelle package.

Acknowledgements

We gratefully acknowledge the cooperation of ESO staff. In particular, this work benefited from discussions and correspondence with D. Baade and D. Ponz. The calibration spectra in the red were provided by J. Melnick. The MIDAS reductions were performed using the facilities at ESO-Garching. H. Van Diest (KSB) helped in introducing software changes in IHAP for test purposes in Brussels. The Belgian Nationaal Fonds voor Wetenschappelijk Onderzoek is acknowledged for a grant in connection to this work (nr. S2.0091.88).

References

D'Odorico, S., Ponz, D.: 1984, *The Messenger* **37,** 24.

Goodrich, R.W., Veilleux, S.: 1988, *Publ. Astron. Soc. Pacific* **100,** 1572.

Norlén, G.: 1973, *Physica Scripta* **8,** 249.

Palmer, B.A., Engleman, R.Jr.: 1983, *Atlas of the Thorium Spectrum,* Los Alamos National Laboratory, ed. H. Sinoradzky.

Pushing CASPEC to the Limit

E.J. WAMPLER, ESO

Recent CASPEC users will have noticed that there is a continuing programme to upgrade the capabilities of the spectrograph. Together with electromechanical modifications of the spectrograph itself, there have been changes in the data reduction procedures. In addition, there is now substantially more experience with the biases that ESO reduction techniques introduce into the data. These improvements and the increased understanding of the critical processes can lead to a substantial increase in the limiting magnitude of CASPEC over that obtained in the past. Here I want to discuss some of the important choices to be made if good signal-to-noise (S/N) ratios, together with high resolution, is needed for faint objects. A general description of CASPEC has been given by D'Odorico et al. (1983).

The detector now used with CASPEC is RCA CCD number 8. This CCD has a readout noise equal to about 25 e^- when it is used with its controller operating at high gain. When observing faint objects, the CCD controller should be operated at the highest possible gain since faint sources do not tax the dynamic range of the system and a small step size in the analogue to digital conversion of the data reduces quantization errors when working at low signal levels.

CCD number 8 has several cosmetic and operational problems that affect its ability to detect weak signals. Between columns numbers 1 and 40 the background drops with increasing column number. Column numbers 40–45, 161 and 201 are always bright and must be discarded. For approximately 48 hours after the CCD has first been turned on, the dark current is high, initially as much as one hundred times the 2-3 $e^- pix^{-1} hour^{-1}$ that is reached after a few days of operation. Therefore, observational programmes that are directed to the spectra of objects fainter than about mag 15 should be scheduled after programmes for brighter stars. CCD number 8 has some UV sensitivity but the sensitivity below about 4300 Å drops rapidly. It is possible to reach magnitude 14 or 15 at 3700 Å with a S/N ratio of about 50 after an integration time of several hours. At 5000 Å the gain in limiting magnitude over that at 3700 Å is about 2 magnitudes.

Even though the readout noise of CCD number 8 is lower than that of ESO's other RCA CCDs, this readout noise is still the dominating noise source when faint objects are observed. Therefore, the S/N ratio that can be achieved is directly proportional to the integration time rather than the square root of the integration time as is the case when the limiting noise source is not the detector noise. I have used integration times as long as 5 hours when observing faint sources. Such long integration times do result in a large number of cosmic ray events. However, the situation is not as bad as it may first appear; CCD number 8 is a high resolution CCD and the small, 15 μm square, pixel format greatly aids the identification and removal of cosmic ray events. Figure 1 shows the results of removing cosmic ray noise from CCD exposures on the 16.5-mag quasar UM402 = Q 020207-003. Figure 1a shows a three-hour frame before cleaning. In Figure 1b the lower threshold of the image was set to 280 DN, just above the highest level reached by the quasar signal. In Figure 1b nearly all the cosmic ray events are seen. Despite the large number of cosmic ray events seen in the figure, only about 1% of all image pixels are affected by these cosmic rays. Filtering programmes, if used with a fixed threshold set to 280 DN (just above the highest level of the quasar signal), can be very effective in removing the cosmic ray tracks seen in this image. The cosmic ray impacts on the CCD generate a large number of electrons but these do not migrate very far in the Si substrate. The influence of a cosmic ray impact is confined to only a few pixels. Because these pixels are small, the contrast between the cosmic ray events and the photon signal from the spectrum is large. Leach (1988) has measured the cosmic ray e^- generation in CCDs. He finds that the differential pulse height distribution of cosmic ray generated electrons has a peak at about 400 e^-. This distribution is very skewed to high energy events; only a small fraction of all events produce fewer than 400 e^-.

The ESO RCA CCDs also show events caused by a local source of radioactivity. At least for CCD number 8, the local source has a pulse height distribution that is similar to that of the cosmic rays. An examination of the detected radiation events seen on long exposure frames taken with CCD number 8 indicates that aside from differences in the total counting rate, the cosmic ray model of Leach (1988) ade-

Figure 1: ***a*** *(upper) A three-hour exposure of the 16.5-mag quasar UM 402. The intensity scale of this frame is in the range 200 < DN < 260.* ***b*** *(middle). The same frame as the upper one but with the intensity scale in the range 280 < DN < 290. This image clearly shows the cosmic rays "hits" accumulated during the three-hour exposure.* ***c*** *(bottom). The average of two three-hour exposures after the images were cleaned as described in the text. Several absorption lines are identified.*

quately describes the radiation events found in CCD number 8 images. After experimenting with alternative programmes for removing these events from the image, the MIDAS programme called "MEDIAN/FILTER" was used since, with a suitable choice of parameters, this programme is effective in removing the cosmic ray events while doing minimal damage to the underlying data.

Figure 1c shows the average of two three-hour integrations; clearly, the effects of the cosmic rays have been largely suppressed. The location of strong features due to CII and NV lines are indicated together with the weak CII fine structure transition. It is noticeable that the residual intensity in the centre of the CII line is very low. After data reduction this intensity was found to be less than 5%. Figure 2 shows a plot of the data in the neighbourhood of the CII line after extraction and wavelength calibration but before any correction for the sky or scattered light background was made. The scattered light properties of CASPEC are quite reasonable.

In order to improve the stabilization of CASPEC, a mechanical grip has been installed to clamp the cross disperser, which in the past has been held in position by an active servo system that had a small amount of jitter.

When CCD number 8 is used with CASPEC, a single pixel corresponded to 0.36 arcsec perpendicular to the dispersion and 0.56 arcsec along the dispersion. With the 31.6 groove mm^{-1} grating the spectral resolution represented by a single pixel was about $R \equiv \lambda/\Delta\lambda$ = 65,000. Although the optics of the spectrograph are nearly good enough to actually achieve this resolution, atmospheric seeing, guiding errors and the need to oversample the image reduced the resolution. For the UM 402 observations a 1.8 arcsec wide slit was used, but the seeing during the observing period was equal to, or less than, one arcsec. This gave a resolution approaching R = 30,000. The narrowest lines seen in the spectrum of UM 402 suggest that the velocity resolution exceeded 15 km s^{-1} (R = 20,000).

The 3.6-metre telescope was guided using a TV guiding system locked to an offset guide star. To monitor the guiding, a mirror was periodically inserted behind the spectrograph slit to relay transmitted light to a second camera that gave a display of the quasar image in the slit. The position of the offset guider was adjusted from time to time to remove the effects of differential flexure between the guide probe and the spectrograph and to accurately maintain the centring of the quasar image in the spectrograph slit. For faint objects, wide slits should be used in order to pass as much starlight as possible into the spectrograph. It is important to check the centring of a faint star by seeing the light transmitted through the slit. The CASPEC slit jaws do not have good edges. If the star is slightly off centre, it is possible to lose a substantial amount of light on the rounded edge of the slit jaw without seeing the lost light when viewing the image of the slit face.

Experiments showed that for observations in the declination range $+10 > \delta > -40$ and with the entrance slit oriented along the East-West direction, the principal component of internal spectrograph flexure displaces the spectrum perpendicular to the dispersion. The amount of this flexure can be reduced by rotating the spectrograph 180 degrees at meridian passage. Differential atmospheric refraction can shift the position of the blue image of the quasar in the slit relative to that of the green image detected by the TV camera system. Systematic shifts of several km s^{-1} between the two ends of the spectra are possible. If the spectro-

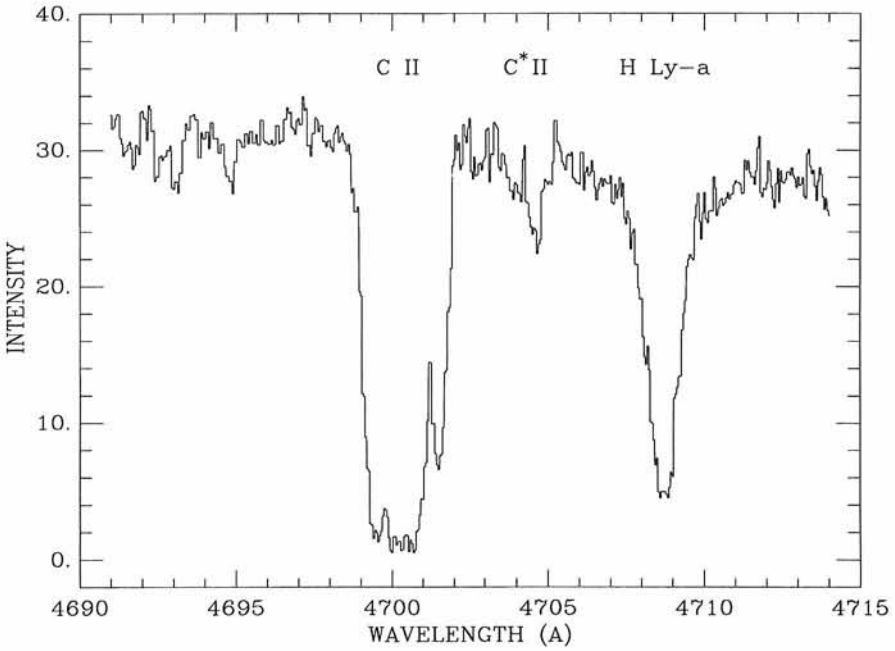

Figure 2: *An extracted portion of the spectrum shown in Figure 1c. Note the residual intensity from scattered light in the bottom of the saturated CII line.*

graph is rotated at meridian passage in order to reduce the total flexure, and if the observations are centred on meridian passage the principal result of this shift is to smear the violet end of the spectrum, rather than to create a systematic wavelength dependent velocity shift.

The wavelength calibration is obtained from observations of a Th-Ar lamp. In the reduction process 50 to 70 spectral lines were used to determine the calibration of each echelle order. (Over 10^3 lines are used for wavelength calibrations in the blue green spectral regions). The use of many lines strongly constrains the two dimensional wavelength fit and, to some extent, reduced the calibration errors caused by line blends and misidentifications in the Th-Ar wavelength table. The wavelength calibration process is an iterative one: the first step is to obtain an initial calibration using only the strongest lines. This initial calibration is then used to constrain a second calibration that uses much weaker spectral lines. If the weak lines are used initially, the programme usually finds an incorrect solution for the line fit. But if the wavelength calibration is done correctly, the mean residuals to the fits are about 9 mÅ in the blue and 12 mÅ in the yellow. In each case this is about ⅟₇ pixel or about 0.7 km sec^{-1}.

The motion of the earth can also result in a differential velocity shift of several km s^{-1} between the beginning and the end of a long integration. The principal effect on the spectrum of the observatories changing velocity vector in space is a reduction of the spectral resolution. A careful choice of the time of observation can mitigate this problem.

If it is intended to convert the observed wavelengths to vacuum values, the formula given by Allen (1964) for the refractive index of air can be used. His formula is valid for standard temperature and pressure and is not strictly correct for the high altitude conditions at La Silla. The difference can amount to about 20 km s^{-1}. The differential effect is approximately 400 m s^{-1} between 4000 Å and 6000 Å.

An important feature of the MIDAS extraction programme is that it rebins the raw image pixels to a uniform wavelength scale before merging individual spectral orders. In order not to degrade the spectral resolution of the extracted spectrum, software bin widths of 0.05 Å can be chosen for the blue spectrum, and for the red 0.10 Å bin widths were used. Both of these choices result in bins that are narrower than the wavelength span of a single CCD pixel. Unfortunately, the rebinning substantially increases the apparent noise in the spectrum. A discussion of "pattern noise", but in a slightly different context, is given in a paper by Dick et al. (1989). The reduction procedure could be improved if the original CCD pixel width was retained. This would result in a non-uniform wavelength spacing of the pixels. At present, with the available software, this is not possible. Rebinning to a coarser grid than the CCD pixel smooths the data but at the expense of lowering the resolution of the spectrum. I think that some of the even pixel, odd pixel jitter in the spectrum seen in Figure 2 is due to this rebinning pattern noise.

I hope that some of these comments prove useful to the CASPEC user communitiy. A total system efficiency of about 4 % can be obtained when using CASPEC! This is rather good for the present state of instrument development. New detectors are on the way, and new instruments and telescopes will make our existing facilities seem modest. But for now CASPEC, if used intelligently, is a powerful tool for widening our understanding of the Universe.

References

Allen, C.W. 1964, *Astrophysical Quantities* (London: The Athlone Press), p. 144.

Dick, J., Jenkins, C. and Ziabicki, J. 1989, *Pub. Astron. Soc. Pac.*, **101,** 684.

D'Odorico, S., Enard, D., Lizon, J.L., Ljung, B., Nees, W., Ponz, D., Raffi, G. and Tanné, J.F. 1983, *The Messenger*, **33,** 2.

Leach, R.W. 1988, *Pub. Astron. Soc. Pac.*, **100,** 853–858.

More Light Through the Fibre: an Upgrading of the Link 3.6-m – CES

S. D'ODORICO, G. AVILA and P. MOLARO, ESO

1. The Configuration of the Fibre Link Today

Different types of commercial fibre optics find useful application in modern astronomical instruments. ESO has been particularly interested in the use of fibres as "light pipes" to feed spectrographs at a distance from the telescope. This is the case of the Coudé Echelle Spectrograph (CES) fed through a 35 m long fibre from the Cassegrain focus of the 3.6-m telescope, alternatively to the standard use with the CAT telescope. The gain one can achieve by using the larger telescope can be as large as two magnitudes over a wide spectral range and this difference opens the way to an entirely new class of observations that at the CAT would be photon limited. Obviously, would-be observers have to be aware that when the link operates, both the CAT and the 3.6-m need to be "booked". As a consequence, the OPC checks with special care whether the use of the larger collecting area is indeed absolutely necessary. A very convincing case and an outstanding scientific justification are a must for these programmes.

ESO observers have access to this new observing mode as of April 1988. A complete description of the set-up had been given in the article by Avila and D'Odorico in the Proceedings of the ESO Conference on "Very Large Telescopes and their Instrumentation", p. 1121 (1988). In March 1989 the system was upgraded and we report here on the options which are now available and on the overall efficiency. This information complements what can be found in the March 1989 version of the Operating Manual of the CES.

There are now four fibres permanently installed between the Cassegrain cage of the 3.6-m telescope and the entrance to the CES. Table 1 summarizes the characteristics of the four fibres. Two types of lenses are used on different fibres to image the pupil of the telescope on the fibre input face and change the input ratio from F/8 to around F/3. The rod lenses have a better transmission below 4000 Å, the self-foc lenses are slightly more efficient between 5000 and 10000 Å. The transmission of the Polymicro and GFO fibres are approximately equivalent (see Fig. 1); both are used with a 3.4 arcsec diaphragm at their entrance. The smaller core diameter QSF fibre is used with a 2.4 arcsec diaphragm: it has no transmission below 4000 Å, but it is more efficient than the other two types above 7000 Å. Three new image slicers are